Date: September 20, 1988

TITLE: Heat Transfer Investigations in a Slurry Bubble Column

PI: S. C. Saxena

INSTITUTION: Department of Chemical Engineering, University of Illinois at Chicago, Box 4348, Chicago, IL 60680
(312) 996-2341

CONTRACT NO.: DE-AC22-86PC90008

PERIOD OF PERFORMANCE: September 3, 1986 through September 20, 1988

OBJECTIVE: To investigate the heat transfer characteristics in two slurry bubble columns (10.8 and 30.5 cm diameter) equipped with heat transfer probes of different sizes and configurations as a function of system and operating parameters.

TECHNICAL APPROACH: The 10.8 cm diameter Plexiglas slurry bubble column along with its associated units viz., the air supply system, slurry circulation loop, temperature and pressure measurement systems, on line data acquisition and analysis system, heat transfer probes and probe bundle, is completely functional and a variety of measurements have been completed. The air holdup in air-water system is measured for increasing and decreasing air velocities, in semi-batch and continuous modes of operation. Similar measurements are taken for the three-phase systems where glass beads and red iron oxide particles of different sizes are used as the solid phase. These hydrodynamic data are compared with the predictions of various correlations available in the literature.

The heat transfer coefficient for an immersed single probe of 19 mm outer diameter and two-and three-phase dispersions are measured as a function of air velocity, solids concentration and particle diameter. It is found that the effect of solids concentration on heat transfer coefficient is sensitively dependent on particle diameter.

The installation and testing of the larger 30.5 cm diameter slurry bubble column is completed and heat transfer and holdup data have been taken for the air-water system as a function of air velocity. Work with three-phase systems is in progress.

The local temperature of a probe element is measured as a function of time for various recording speeds of 20 to 200 readings per second. These temperature history records are being analysed to understand the mechanistic heat transfer process and the roles different phases play in removing heat from the immersed surface in the slurry bubble column.

SIGNIFICANT ACCOMPLISHMENTS: Based on measurements of gas holdup and heat transfer coefficient under varying conditions several important conclusions have been drawn. These are: (a) the gas holdup depends uniquely not only upon the value of the air velocity but also how this value is approached and whether or not the liquid is stationary or moving, (b) the existing seven sets of heat transfer data for the air-water system have serious disagreements and the new data have helped in resolving many of the discrepancies, and (c) our measurements have indicated that even the qualitative variation of heat transfer coefficient in bubble column with solids concentration in the slurry depends on the size of the solid particles.

PUBLICATIONS: (1) S. C. Saxena and R. Vadivel, Heat Transfer from a Tube Bundle in a Bubble Column, Int. Commun. Heat Mass Transfer 15, 657 (1988); (2) S. C. Saxena, R. Vadivel and A. K. Verma, Heat Transfer and Hydrodynamics of Bubble Columns with Internals, Proc. Third Latin American Congress on Heat and Mass Transfer, Guanajuato (Mexico), to be published; (3) S. C. Saxena and A. K. Verma, Transport Phenomena in Multiphase Reactors, Proc. Int. Conf. on Advances in Chemical Engineering, IIT Kanpur (India), to be published; (4) S. C. Saxena, Heat Transfer from a Cylindrical Probe Immersed in a Bubble Column, Chem. Eng. J., under review; (5) S. C. Saxena, A. K. Verma and A. C. Saxena, Heat Transfer from a Cylindrical Probe in a Slurry Bubble Column, Int. Commun. Heat Mass Transfer, under review, and (6) S.C. Saxena, R. Vadivel and A.C. Saxena, Hydrodynamic and Heat Transfer Characteristics of Bubble Columns Involving Fine Powders, Powder Technology, under review.

INTRODUCTION

The main goal of this research program is to generate a good data base so that the phenomenon of heat transfer from immersed surfaces in slurry bubble columns may be understood in relation to the indirect coal liquefaction technology. In doing so it is imperative that the data be generated for heat transfer coefficient between immersed surfaces of heat exchangers of different sizes and configurations and three-phase dispersions involving a variety of fluids and solids of different sizes and thermophysical properties covering a range of operating variables viz., gas and liquid velocities, temperature, slurry concentrations etc. To accomplish this two bubble columns have been set up and thoroughly instrumented for temperature, pressure, gas and liquid velocity measurements. The design of the 10.8 cm diameter slurry bubble column along with all the support units was presented[1] at the indirect liquefaction contractors' review meeting. The installation, testing and some of the initial results of gas holdup and heat

transfer coefficient were described in a subsequent presentation[2]. This paper also included the partial design, fabrication and installation of a larger 30.5 cm diameter larger slurry bubble column. This unit in particular will enable measurements over a temperature range covering from ambient to 550K and for a variety of tube bundles containing varying number of heat transfer probes.

Both these slurry bubble column facilities are functional and during the last year several two-and three-phase systems have been examined, and hydrodynamic and heat transfer data have been generated. These measurements include air water, and glass beads and red iron oxide particles of different sizes. The holdup data of different phases is examined on the basis of available correlations. The dependence of the heat transfer coefficient on gas velocity, particle size, and solids concentration is determined for air-water, air-water-glass beads, and air-water-iron oxide powders. These results are summarized in this presentation and plans for future work are outlined in this background. The local temperature history of an element of heat transfer surface is recorded to elucidate the mechanism of heat transfer.

SMALLER BUBBLE COLUMN FACILITY

The schematic of the 10.8 cm diameter Plexiglas bubble column with its associated air supply and pressure measurement circuits is shown in Fig. 1 following Saxena and Vadivel[3]. The column is constructed form a 1.27 cm thick transparent Plexiglas tube, 225.4 cm in height comprising of a calming section (14.6 cm), a test section (170.2 cm) and an air disengagement section (40.6 cm). A bubble cap distributor plate for the calming section and a perforated distributor plate for the bubble column are used to ensure uniform distribution of air at the column base. The air is supplied by a 18.65 kW, two-cylinder, two-stage air cooled Curtis compressor equipped with a surge tank, a refrigeration dryer, and three filters. The air line is also provided with a pressure regulator, a rotameter and valves. To measure the pressure profile along the column an elaborate measurement and control system is incorporated as shown in Figure 1. A liquid or slurry circulation loop is also provided to obtain data in the continuous mode of operation.

As heat transfer surfaces, a probe bundle comprising of five 19 mm diameter and 188 cm long Plexiglas tubes in a square arrangement with a pitch of 3.65 cm, and a single 19 mm diameter probe are used in the investigations reported here. The details of these probes are shown in Figures 2 and 3 following Saxena, Vadivel and Verma[4], and Saxena [5]. The design details of the single tube heat transfer probe are displayed in Figure 2A. Basically it consists of three sections, top, middle and bottom, put together by two delrin connectors 50 mm long. The Teflon bottom section is 305 mm long and has a conical end taper to enable a smooth liquid flow around it. A threaded connector connects the bottom section to the middle brass section. Inside the brass rod a calrod heater (305 mm) is inserted and this middle

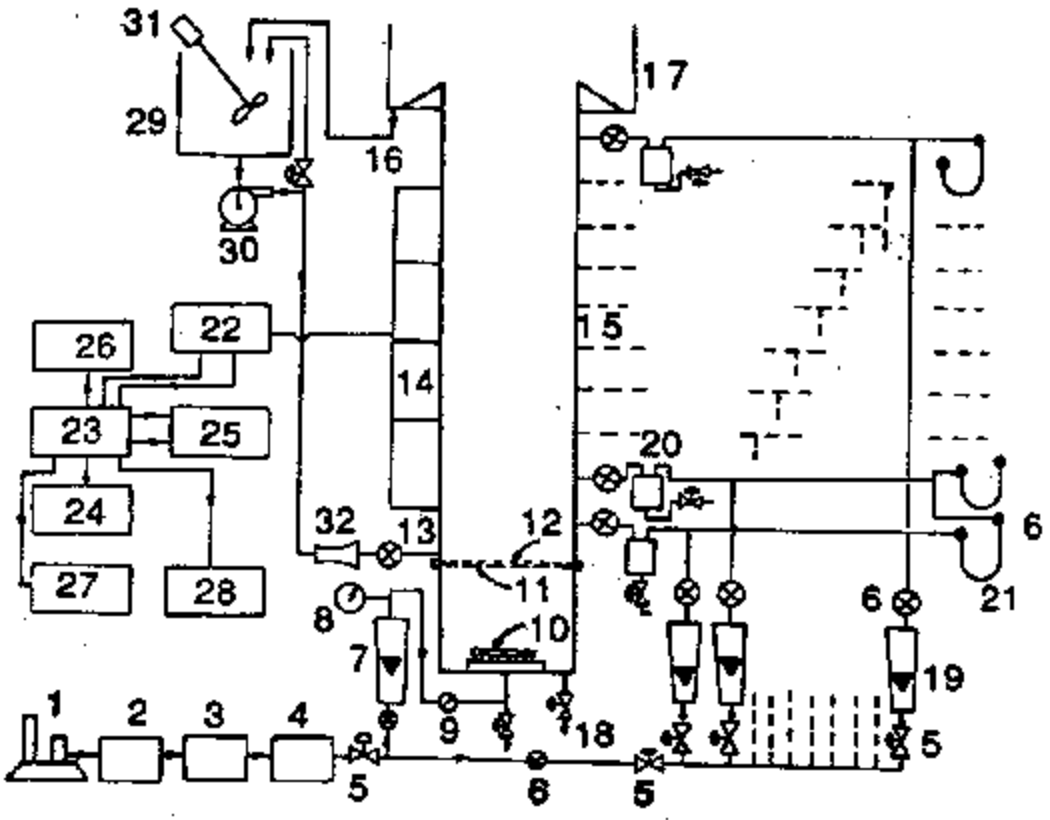

Fig. 1. Schematic of the 10.8 cm diameter bubble column along with air supply loop, temperature and pressure measuring circuits and liquid circulation loop: (1) air compressor, (2) surge tank, (3) refrigerator drier, (4) oilscer filter, (5) pressure regulator valves, (6) gate valves, (7) rotameter, (8) pressure gage, (9) one-way valve, (10) bubble cap distributor, (11) perforated-plate distributor, (12) stainless steel wire cloth, (13) water inlet, (14) thermocouples, (15) Plexiglas column, (16)water outlet, (17) disengaging section, (18) liquid drain, (19) purgemeters, (20) trap bottles, (21) manometers, (22) data acquistionsystem, (23) computer, (24) keyboard, (25) disc drive, (26) monitor, (27) printer, (28) plotter, (29) liquid storage tank, (30) liquid circulation pump, (31) stirrer and (32) venturimeter.

section is connected to the stainless steel tube top section by another threaded connector. An O-ring seal is provided between the connector and the steel tube to avoid any liquid seepage from the column into the tube.

The surface temperature of the brass section of the probe containing the calrod heater is measured by strategically located seven copper-constantan thermocouples. Their orientation and location on the surface is detailed in Figure 2A. Thermocouples 9 and 10, and 8 and 11 are provided to measure the end heat loss to the connectors. A clamp for centrally locating the probe in the column and to damp out its any vibratory motion is fabricated and its design is shown in Figure 2B. The clamp consists of three arms at an angular separation of 120°. The three arms are attached to a central ring clamp (1) which fits tightly on the probe surface with the help of a screw (2). The two arms (3,4) have threaded Teflon rounded caps (5) to provide soft and good grip at the inner column surface (6). The third arm (7) has a telescopic arrangement (8) with a spring (9) and a locking pin (10). The front end (11) of this arm (7) can thus be moved in and out against the spring (9). The three-arm locating clamp will thus hold the probe rigidly along the column axis. Three such clamps are used along the probe length and these have successfully avoided and completely damped any possible vibration of the probe in the column.

The five tube bundle arrangement is shown in Figure 3. The central tube is provided with a 34 cm long brass section containing a 30.5 cm long calrod heater. To measure the surface temperature of this brass section five copper-constantan thermocouples are cemented in milled grooves, 72° apart, and at 5.08, 10.6, 15.24, 20.32 and 25.4 cm from the end. The heater is energized by a HP6274A D.C. power source comprising of a master and two slaves, each providing 0-60V and 0-15A with a power regulation of 0.01 percent. This arrangement of auto-series operation is characterized by one-knob control in the master and the amplitude of the slaves output voltage is equal (or proportional) to that of the master. As shown in Figure 4, a voltmeter and an ammeter enables to establish accurately the power fed to a heater. Five thermocouple probes are installed to measure the bulk column temperature along its height, and also radially at a particular height by moving it in and out. Seventeen thermocouples from these five probes designated as A,B,C,D and E, and five thermocouples for measuring the bulk column temperature through a thermocouple selector switch, are all brought to a Hewlett Packard 3497A data acquisition/control unit with thermocouple compensation as shown in Figure 5. This unit is programmed by a computer (HP310) which also converts the measured voltages to the corresponding temperatures with the help of appropriate software. The system has dual flexible disc drives and allows the computer either to read data stored on the disc or to write data on a disc. Finally, the processed data are displayed on a HP35731A monochrome video and/or recorded on a Think Jet printer. The system also includes a HP7440A eight pen graphics plotter.

For measuring the axial and radial temperature profiles in the column a thermocouple probe is designed as shown in Figure 6. The thermocouple is made from 28AWG copper and constantan wires with glass braid insulation.

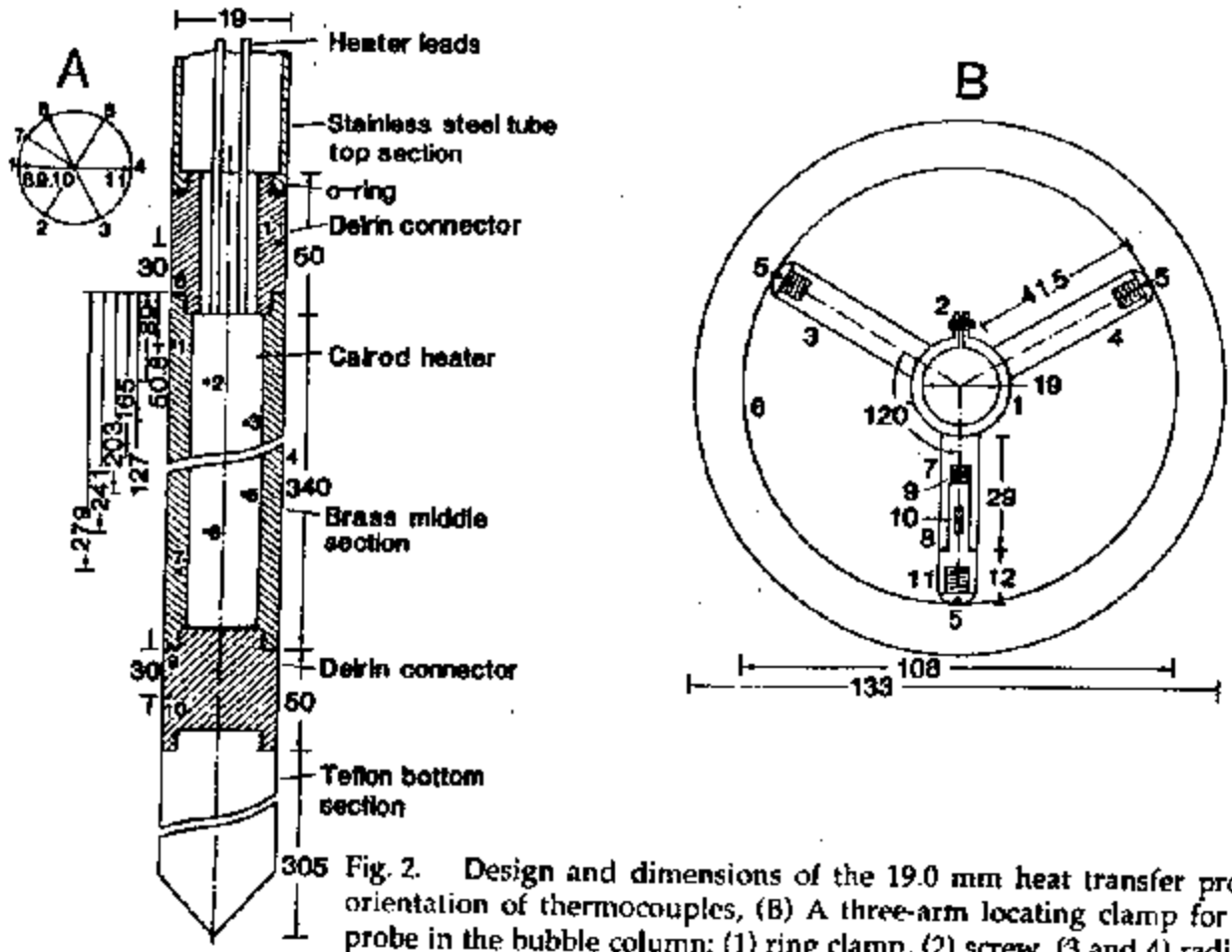

Fig. 2. Design and dimensions of the 19.0 mm heat transfer probe assembly (A) orientation of thermocouples, (B) A three-arm locating clamp for the heat transfer probe in the bubble column: (1) ring clamp, (2) screw, (3 and 4) radial arms, (5) Teflon rounded cap, (6) column surface, (7) telescopic arm, (8) telescopic arrangement, (9) spring, (10) locking pin, and (11) front end of the telescopic arm. All dimensions are in mm.

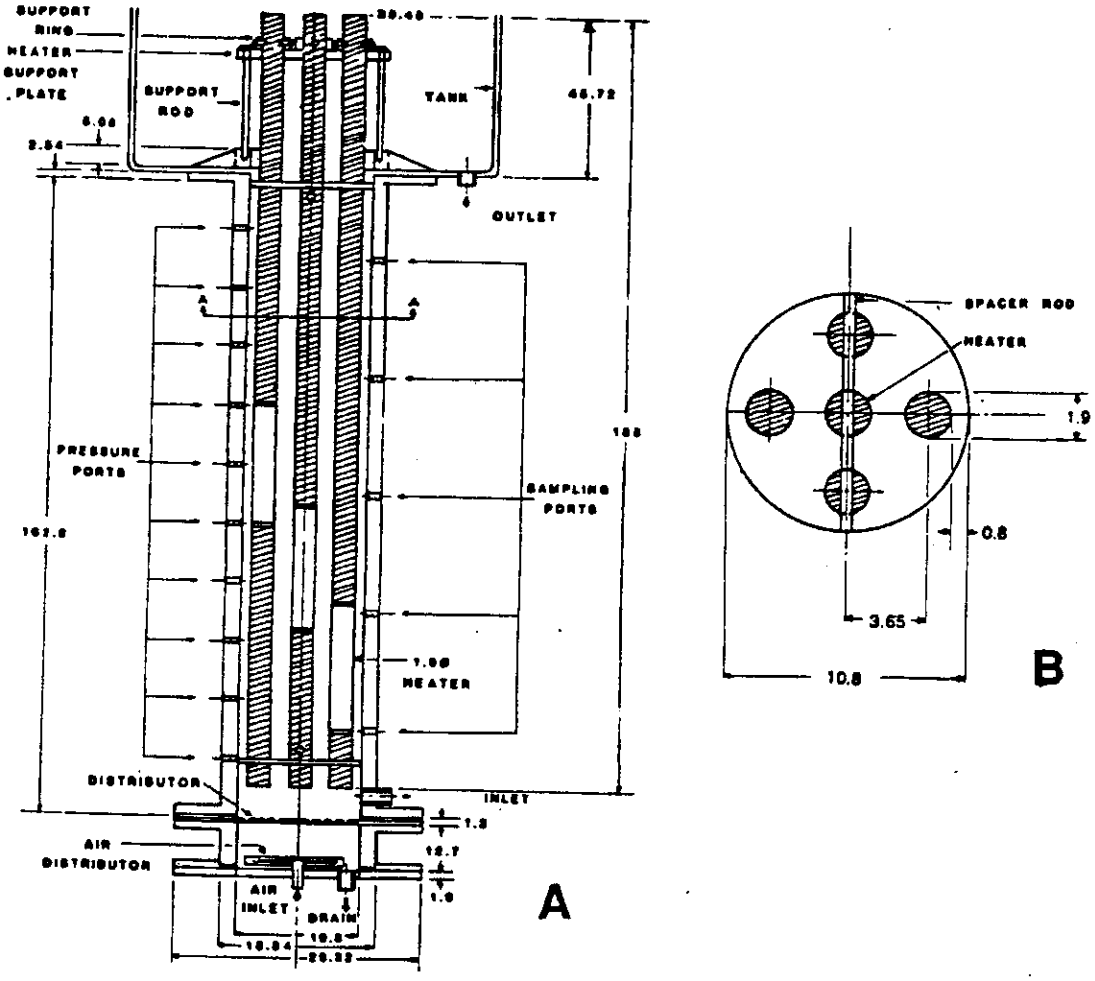

Fig. 3. (A) Schematic of the slurry bubble column and the heat transfer probe bundle drawn not to scale. All dimensions are in cm. (B) Plan view of the section A-A of the column. All dimensions are in cm.

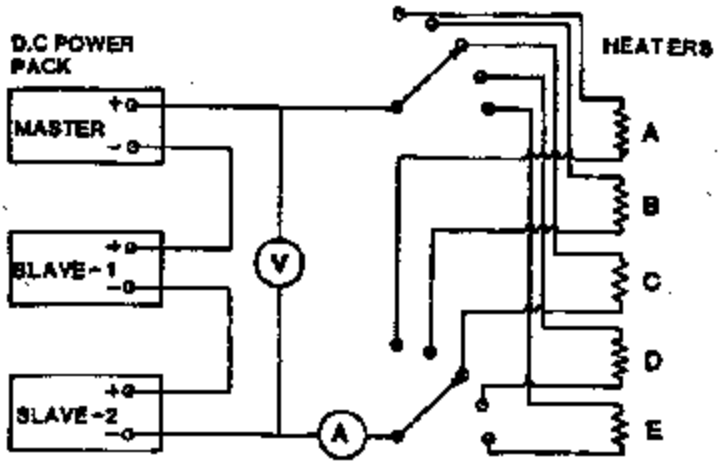

Fig. 4 Schematic of the D.C. power supply for the heat transfer probes.

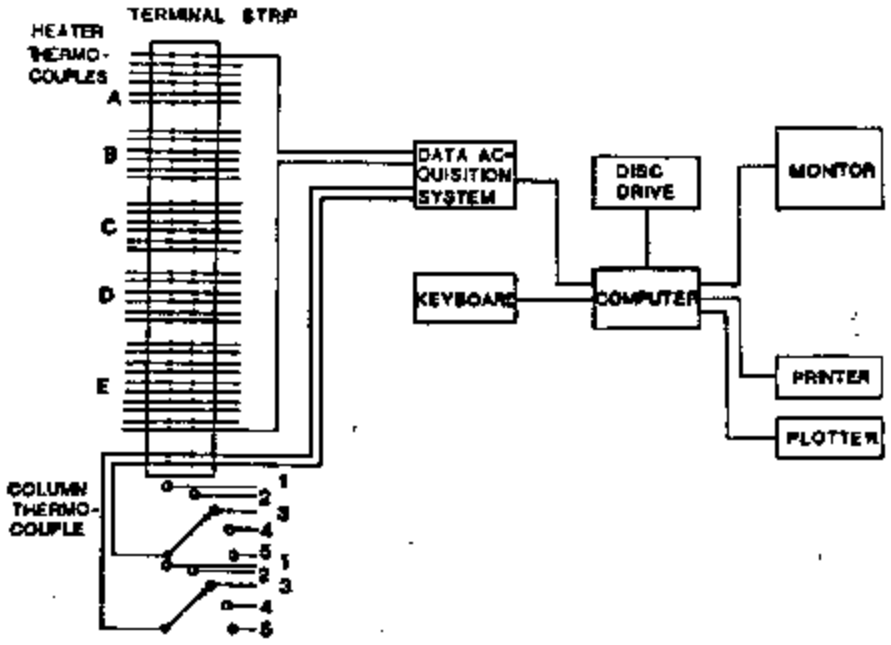

Fig. 5. Detailed schematic of the temperature measuring system.

The thermocouple junction is imbedded in a well on the front face of a specially designed Teflon plug by using copper cement. The plug is force fitted in a stainless steel tube of 6 mm outer diameter, 1 mm wall thickness and 15 cm long. The thermocouple wires are passed through the tube and locked in position at the outer end of the tube by a PVC shrink tube and epoxy cement. The probes can be inserted to various radial positions in the column and locked in position by swagelok connector arrangement as shown in Figure 6.

LARGER BUBBLE COLUMN FACILITY

The schematic of the 30.5 cm diameter bubble column along with its associated air supply system, pressure and temperature measuring circuits is shown in Figure 7. The air supply loop consists of a two-stage air compressor (1), refrigerator drier (2), filter (3), pressure regulator valve (4), rotameters (5), air pressure gage (6), gate valves (7) and one-way valve (8). The pressure measurement system comprises of four trap bottles (17), four purgemeters (18), four liquid manometers (19), pressure sensor (20), pressure monitor (21) and on-off valves (22). The pressure sensor is an Omega PX120-015 GV stainless steel transducer (20) appropriate for the pressure range 0 to 15 psig and capable of handling corrosive media. The output of this transducer is indicated on the pressure monitor (21), and Omega DP-350 digital transducer indicator. A suitable valving arrangement (22) brings this transducer into the desired pressure measuring location. Liquid manometers (19) are also simultaneously exposed for the pressure measurement. The two sets of readings agree with each other within a maximum deviation of 0.2 percent.

Four copper-constantan thermocouples are provided along the height of the column as shown in Figure 7 to provide the vertical radial profile. The design details of these thermocouple probes are similar to those as reported by Saxena[5] and described in the previous section. The output of all these thermocouples is brought to a Hewlett Packard 3497A data acquisition/control unit with thermocouple compensation (23). This unit is programmed by a computer (24), HP310, which also converts the measured voltages to the corresponding temperatures with the help of appropriate software. The system has dual flexible disk drives (26) and allows the computer either to read data stored on the disc or to write data on a disc with the help of HP4620A keyboard (25). Finally, the processed data are displayed on a HP35731A monochrome video monitor (27) and/or recorded on a HP2225 Think Jet printer (28). The system also includes a HP7440A eight-pen graphics plotter (29).

The slurry column consists of four glass sections of total height 300 cm (15), four stainless steel inserts each 7.5 cm high (14), and the bottom conical section (10). These are assembled together on a specially designed metal structure enabling to work around the column at two different levels. A specially designed clamp system is fabricated to attach the flange at the second

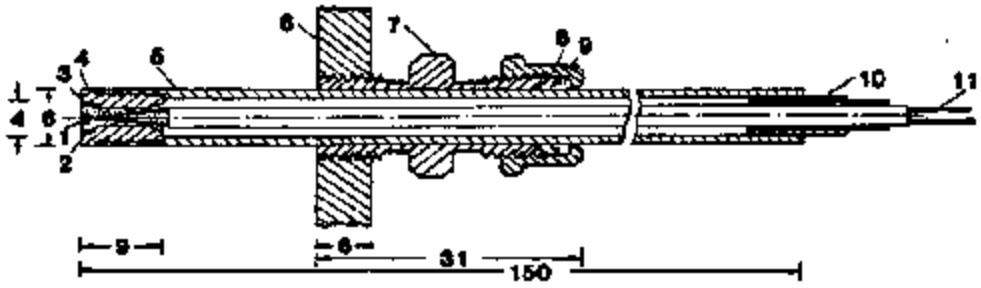

Fig. 6. Design details of the thermocouple probe: (1) copper constantan thermocouple, (2) thermocouple well, (3) copper cement, (4) Teflon plug, (5) stainless steel tube, (6) column well, (7) swagelok connector, (8) front ferrule, (9) back ferrule, (10) shrink tube, (11) thermocouple leads. All dimensions are in mm.

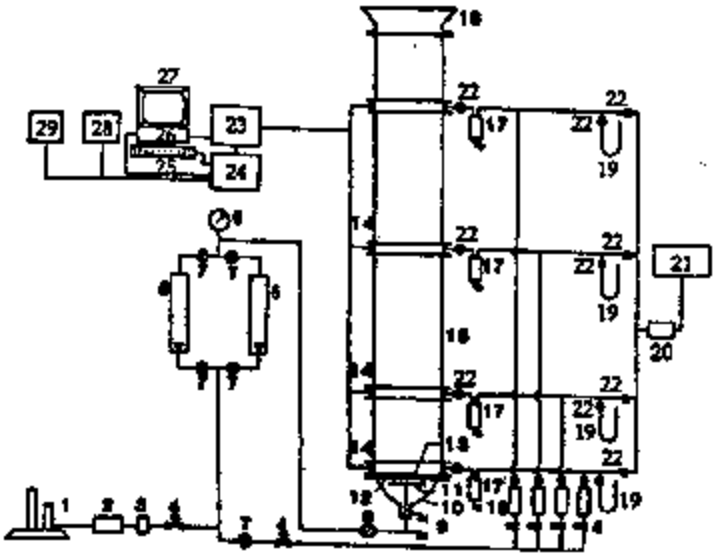

Fig. 7. Schematic of the 0.305 m diameter slurry bubble column along with air supply loop, temperature and pressure measuring circuits. (1) air compressor, (2) refrigerator drier, (3) oilscer filter, (4) pressure regulator valve, (5) rotameters, (6) pressure gage, (7) gate valves, (8) one-way valve, (9) liquid drain, (10) conical section, (11) bubble-cap distributor plate, (12) perforated plate distributor, (13) stainless steel wire cloth, (14) metal inserts, (15) glass column, (16) diverger section, (17) trap bottles, (18) purgemeters, (19) manometers, (20) pressure sensor, (21) pressure monitor, (22) on-off valve, (23) data acquisition system, (24) computer, (25) key-board, (26) disc drive, (27) monitor, (28) printer, and (29) plotter.

metal insert (14) to the support structure. This arrangement absorbs the load of the bottom column section, glass conical section (10), bubble cap distributor plate (11), perforated plate distributor (12) and the liquid drain adapter along with its accessories at the second metal insert from where the entire bottom column assembly is hanging . Similarly, the rest of the upper column section rests and is supported from a specially designed clamping system attached at the second and third metal inserts from the bottom of the column.

The design details of the bubble cap and perforated plate air distributors are shown in Figure 8. The bubble cap distributor (9) is 203.2 mm diameter stainless steel plate having sixty-one bubble caps arranged in concentric circles as shown in Figure 9 with an equilateral triangular pitch of 28.6 mm. This plate is held in the cylindrical section (10) 44.4 mm high and terminating into the support and air inlet pipe (1) of 12 mm internal diameter. The pipe is introduced into the bottom conical section (8) of the column and is made air and liquid tight by attaching it to a specially designed stainless steel liquid drain adapter (3) through a Teflon coated nut (2). The adapter (3) also provides a similar air and liquid tight seal to conical glass section by a flange joint (6) using gasket (5) and a soft insert (7). The adapter also has a liquid drain (4) for removing any liquid that might drain into this section through the distributor plate from the main column. The air distributor square plate (11) is made from a stainless steel plate of 4 mm thickness and 420 mm to a side and has 0.8 mm orifices in a square arrangement of 9.5 mm pitch as shown in Figure 10. A stainless steel 200 X 200 wire cloth is mounted over this perforated plate to avoid solids weeping from the column into the distributor section. Six locating pins (14) are provided in the distributor plate (11) to ensure its correct positioning in the conical section (8). The perforated plate is held in the right position by three spacer studs (13).

The top end of the column is provided with a diverging section as shown in Figure 11. The stainless steel plate (1) of 420 mm in diameter and 4 mm thickness is provided as a cover at the top of the column. It has fifty-seven holes of 25.4 mm diameter arranged in a square configuration with a pitch of 35 mm. The conical diverging section has a neck 50 mm tall and slant height of 150 mm as shown in Figure 11.

A cylindrical heat transfer probe, 19 mm in diameter and 3.25 m long, is axially mounted in the column with the help of three specially designed three-arm clamps. Each clamp has one rigid and two telescopic arms. The details are shown in Figure 12. The heat transfer probe consists of three sections viz., top, middle and bottom. The middle section contains the heated test brass section, 36.1 cm long, and a calrod heater is installed axially inside this brass section. On either side of this test section are the stainless steel sections attached to the brass section by Teflon connectors. The heater leads are brought out and are connected to a regulated HP6274A D.C. power source comprising of a master and two slaves. The lower end of the probe terminates into a conical stainless steel taper to enable a smooth flow around the probe. On the test surface six thermocouples are cemented into milled grooves at various angularly staggered axial positions as shown in Figure 12. To locate the test section at different axial positions in the column, different

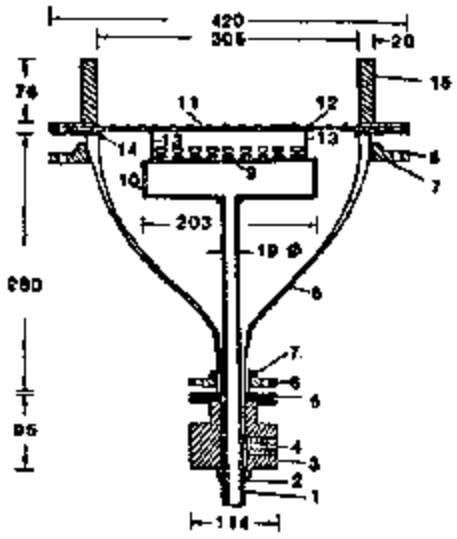

Fig. 8. Design details of the bottom end assembly of the 30.5 cm diameter slurry bubble column. (1) gas inlet pipe, (2) Teflon coated nut, (3) liquid drain adapter, (4) liquid drain, (5) gaskets, (6) flanges, (7) soft inserts, (8) conical glass section, (9) bubble cap distributor plate, (10) cylindrical holder, (11) perforated plate distributor, (12) stainless steel wire cloth, (13) spacer studs, (14) locating pins, and (15) metal insert. All dimensions are in mm.

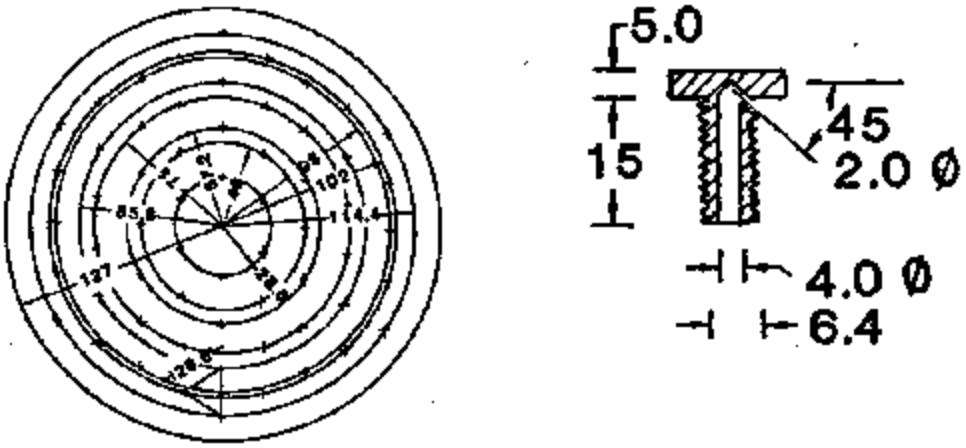

Fig. 9. Arrangement of the bubble-caps on the distributor plate. All dimensions are in mm.

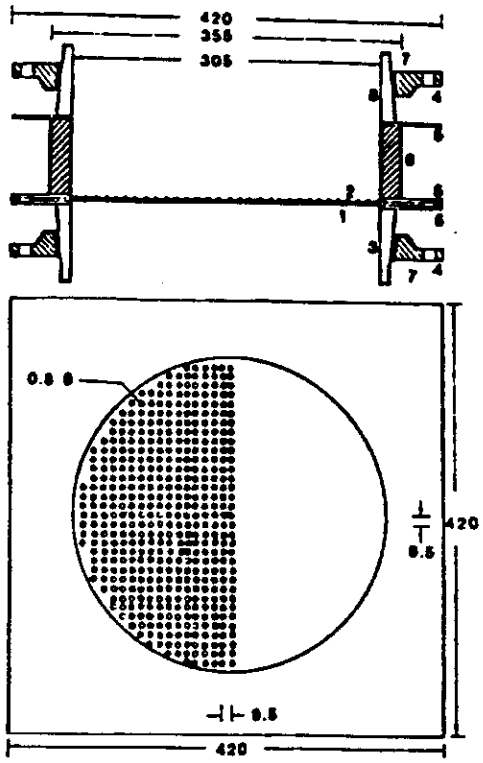

Fig. 10. Design details of the perforated gas distributor plate for the 30.5 cm diameter slurry bubble column. (1) perforated plate distributor, (2) stainless steel wire cloth, (3) bottom conical section, (4) flange, (5) gasket, (6) metal insert, (7) soft inserts, and (8) glass column. All dimensions are in mm.

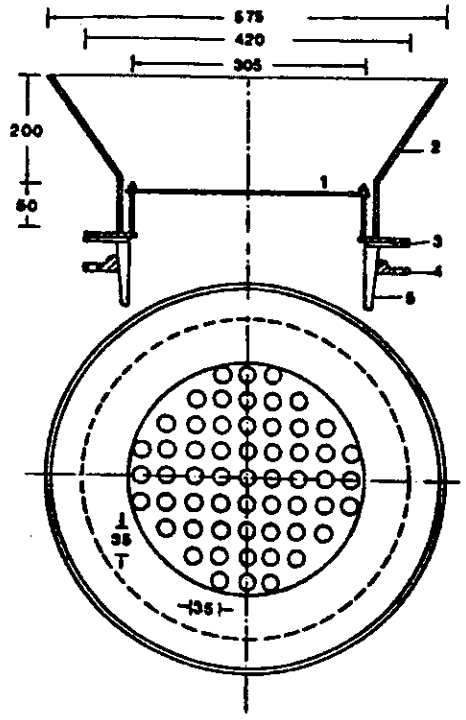

Fig. 11. Design details of the diverger section at the top end of the 30.5 cm diameter slurry bubble column. (1) stainless steel perforated plate, (2) diverger section (3) gaskets, (4) flange, and (5) glass column. All dimensions are in mm.

stainless steel sections of proper lengths are attached on either end. Three different positions are investigated in this work, referred to as the upper, middle and lower regions of the column. In the upper region, the middle of the heated test section is located 218.8 cm above the distributor plate, while its height is 160.5 and 52.3 cm for the middle and lower regions respectively.

To obtain the radial temperature profile in the bubble column a thermocouple probe is specially designed as shown in Figure 13. It is made from an acrylic tube, 9.5 mm in diameter, with eight copper-constantan thermocouples located at 0,2,5,10,20,30,45 and 60 mm from its tip. The length of the probe is 28 cm and is located approximately in the middle of the heated test section and installed in the stainless steel insert with a swagelok connector. It can thus be moved in and out in the column at a given height to obtain the radial temperature profile necessary for the calculation of the heat transfer coefficient between the probe and the dispersion around it as discussed later in the paper.

HYDRODYNAMIC DATA AND DISCUSSION

A series of experiments is conducted to establish the dependence of average ($\bar{\epsilon}_g$) and local (ϵ_g) air holdup on air velocity, U, and water velocity, V. $\bar{\epsilon}_g$ is computed for a given value of V as a function of U by the following relation:

$$\bar{\epsilon}_g(U) = \left[H_e(U) - H_s\right] / H_e(U). \qquad (1)$$

Here H_s is the initial slumped height of the water column and H_e is the expanded height of the air-water dispersion for air velocity U. Such data are taken for cocurrent flow of air and water. Further variance in such data is introduced by variation in the value of H_s, presence or absence of the heat transfer probe (internal) in the column, and whether data are taken for increasing or decreasing values of U. The local air holdup, ϵ_g, at a particular gas velocity, U, and at a particular height above the distributor plate, h, is obtained by measuring the pressure drop, ΔP, across a section of known height, H, of the air-water dispersion and the following relation:

$$\epsilon_g(U,h) = 1 - \Delta P\left[H(\rho_w - \rho_a)\right]^{-1} \qquad (2)$$

where ρ_w and ρ_a are the densities of water and air respectively.

The experimental air holdup data are reported in Figures 14 - 16. In Figure 14 are shown the data taken in the semi-batch mode (water flow velocity is zero) for both increasing (filled circles) and decreasing (unfilled circles) air velocities. In the former, the air velocity is steadily increased to the desired value in steps and the height of the air-water dispersion is brought to a fixed value (170.12 cm) and thereafter the air flow is instantly stopped and the settled height of the dispersion is recorded and is computed from eqn. (1). Similar data are taken for decreasing air velocities except here first the air

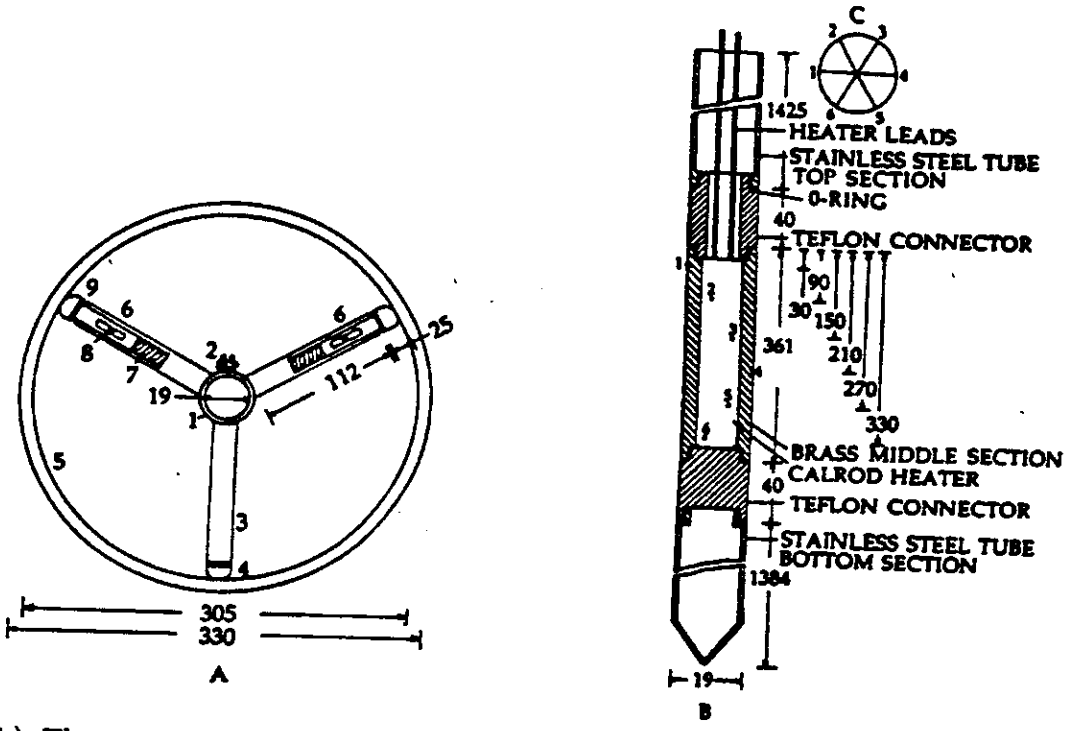

Fig. 12. (A) Three -arm locating clamp, (B) single heat transfer probe, (C) orientation of thermocouples for the 0.305 m diameter bubble column. All dimensions are in mm. (1) ring clamp, (2) screw, (3) radial arms, (4) Teflon rounded cap, (5) column surface, (6) telescopic arms, (7) spring, (8) locking pin, and (9) front end of the telescopic arm.

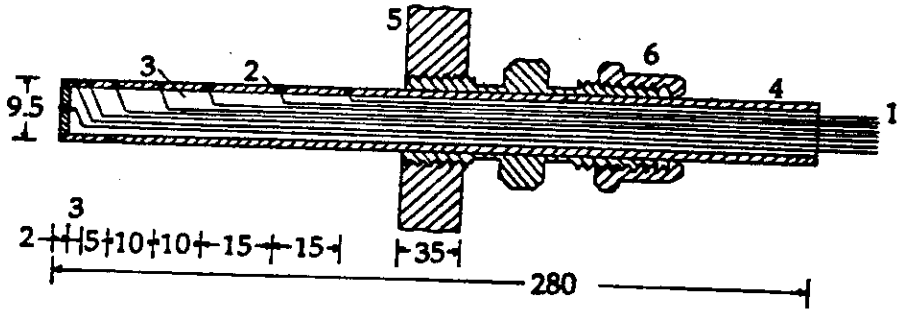

Fig. 13. Design details of the radial thermocouple probe. (1) copper-constantan thermocouples, (2) thermocouple well, (3) Silicone rubber (4, acrylic tube, (5) column wall, and (6) Swagelok connector., All dimensions are in mm.

velocity is increased in steps and brought to the maximum value, and thereafter the air flow is decreased in steps and at each step the makeup water is added to bring the dispersion height to 170.12 cm. At the first sight, the data of Figure 14 show considerable scatter but several trends are obvious and these are discussed below.

In most of the runs a pronounced maximum and minimum is observed for increasing air velocity while a monotonic variation of increasing $\bar{\epsilon}_g$ with increasing U is found for decreasing air velocity. This hysterisis effect has been observed by other workers [6-9] and is primarily due to the formation and accumulation of foam at the top of air-water dispersion and secondarily due to foam accumulation in the column. Maruyama et al. [7] based on their work in a two-dimensional column with a rectangular cross-section of 30 cm by 1 cm and a height of 130 cm have attributed such a dependence of $\bar{\epsilon}_g$ on U to different liquid flow patterns. Three regimes of operation viz., uniform bubbling, transition and liquid circulation have been proposed and these are encountered as the air velocity is increased. In the transition regime local liquid circulation near the side walls and gross liquid circulation may occur depending upon the air velocity. At the maximum holdup, a symmetrical two-loop circulation pattern, upward near the middle and downward near the side wall, is observed. A monotonic decrease in $\bar{\epsilon}_g$ is observed when the air velocity is decreased. The magnitude and the nature of $\bar{\epsilon}_g$ variation with U also depends significantly upon the presence of surface active impurities which control the degree of foam formation. Their concentration in distilled water in present experiments also depended upon the duration of the total operation time. In some runs the nonmonotonic variation of $\bar{\epsilon}_g$ with decreasing U, and monotonic variation for increasing U were also found. These results were always consistent with the presence or absence of foam respectively in the column. Experiments with different H_s values in the range (70-99 cm) indicated that $\bar{\epsilon}_g$ is only a weak function of H_s, Saxena et al.[4]

The foam formation is minimized for runs conducted in the continuous mode when air and water are in cocurrent flow. A representative data set is shown in Figure 15 for discrete values of V as a function of U. Not only the variation of $\bar{\epsilon}_g$ with U is monotonic but the hysterisis effect is also absent. No formation or accumulation of foam was visible. For this range of V (0 to 1.2 cm/s) the influence of water flow velocity on air holdup is found to be negligibly small. This conclusion is also substantiated by other measurements. [4,10]

In Figure 16 are plotted the values of ϵ_g along the column height for various decreasing air velocities without (A) and with (B) the heat transfer probe in the column. The two sets of data are found to be in general agreement with each other and this is not surprising in view of the small

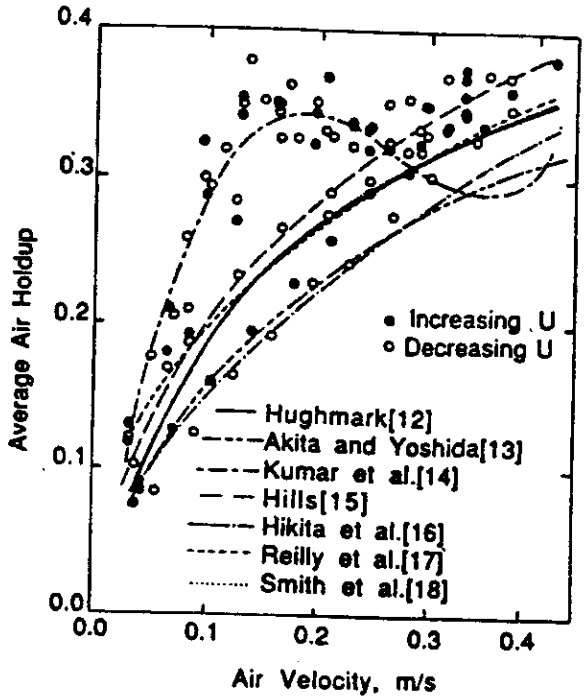

Fig. 14. Comparison of experimental average air holdup data as a function of air velocity with the predictions based on different correlations at 295K.

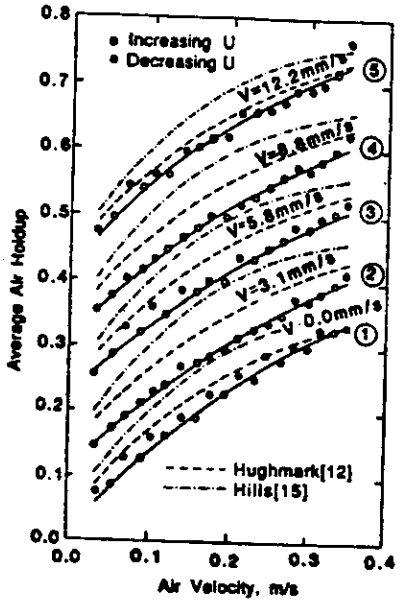

Fig. 15. Variation of average air holdup as a function of air velocity for different water velocities (V) in the column at 295K. For comparison predictions based on two correlations are also shown.

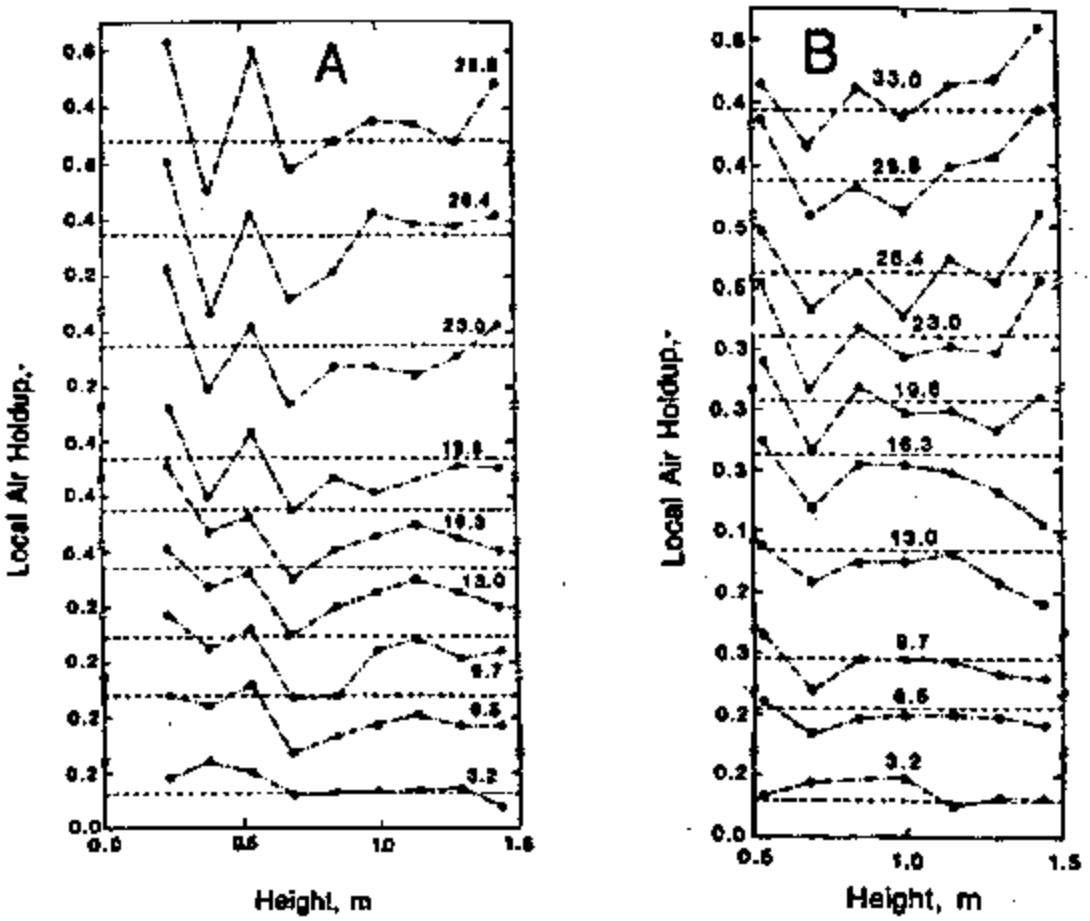

Fig. 16. Variation of the local air holdup as a function of decreasing air velocity at different heights of the water column at 293K. (A) without and (B) with heat transfer probe in the column. Dashed lines represent average air holdup.

cross section of the probe relative to that of the column (about 4 percent). Certain qualitative trends in the ϵ_g values are evident and these may be interpreted to infer the nature of bubble dynamics in the column. In the lower section of the column h < 50 cm, the bubble coalescence becomes increasingly pronounced as the air velocity is increased. This behavior causes the air holdup to decrease with increasing U in this region of h < 50 cm. For 50 < h < 100 cm, the air holdup is relatively constant over the entire air velocity range. For the column region 100 < h < 150 cm, the air holdup increases with h, the increase being more pronounced for higher air velocities. This is attributed to the foam formation the column. It is also clear from these plots that the formation and breakup of foam takes place in the major portion of the column, h > 50 cm, and more so for higher gas velocities. The $\bar{\epsilon}_g$ values are also shown in this figure by dashed horizontal lines and these highlight the departure in the values of ϵ_g from $\bar{\epsilon}_g$ values.

The uncertainty associated with the determination of average air holdup is about 4% at the highest gas velocity and decreases with decrease in gas velocity, being about 0.5% at the lowest gas velocity. The uncertainty of the local air holdup is dependent on the air velocity as well as on the value of the air holdup. At the top end of the column, the air holdup is large due to foam formation and the pressure difference uncertainty is relatively large because of the small magnitude of the pressure difference. The uncertainty is estimated to be ± 50 percent at the highest air velocity. In the remaining portion of the column the uncertainties are ±5 and ±35 percent for the lowest and the highest air velocities respectively.

The knowledge of holdup for the three phases is essential to interpret and characterize the column behavior. These can be determined rather easily by performing the run in a definite order. The column is filled with distilled water up to a stagnant or slumped height of H_L. Next, a known amount of solids is added to the column and the column height of the slurry, H_{SL}, is noted. The air at the desired flow rate is bubbled through the column and the expanded height of the slurry, H_T, is noted when the steady state is reached (about fifteen minutes). The average holdup values of gas, solid and liquid are determined from the following relations:

$$\bar{\epsilon}_g = (H_T - H_{SL}) / H_T, \tag{3}$$

$$\epsilon_s = (H_{SL} - H_L) / H_T = (1 - \bar{\epsilon}_g)(H_{SL} - H_L) / H_{SL}, \tag{4}$$

and

$$\epsilon_L = (H_L / H_T) = 1 - \bar{\epsilon}_g - \epsilon_s. \tag{5}$$

The holdups are measured for decreasing values of the air velocity with the heat transfer probe present in the column. In other words, the air velocity is increased to its maximum value and H_T is recorded, and thereafter the air velocity is decreased continuously in steps and corresponding H_T values are noted. Computed values of $\bar{\epsilon}_g$, ϵ_s and ϵ_L as a function of air velocity for

specific values of C_s for the slurries of three particles are shown in Figure 17. C_s is defined as the ratio of the mass of solids to the volume of the slurry.

The experiments with glass beads having an average diameter of 50.0 μm are conducted with an initial water column height of 85.0 cm in the air velocity range of 3.35 to 35.3 cm/s. Computed values of the phase holdups are displayed in Figure.17A for the solids concentration of 108 kg of solids/m^3 of slurry by curve 2. Curve 1 in this figure corresponds to the case of $C_s = 0$ i.e., two-phase air-water system. Air holdup variation with air velocity for both the cases (C_s = 0 and 108) is nonmonotonic and is due to the formation and destruction of foam in the system as the air velocity is increased. The presence of glass beads increases the air holdup in the foaming regime at lower air velocities and decreases the air holdup in the nonfoaming regime at higher air velocities. Water and glass beads phase holdups follow this characteristic variation of air holdup as the air velocity is increased. Measurement of holdups for the largest size glass beads are conducted for four values of C_s; 0, 104, 214, and 312 kg of solids/m^3 of slurry and results are displayed in Figure 17C. The qualitative trends are similar to those found for the smallest particle (50 μm). The increasing concentration of glass beads in the system tends to suppress the formation of foam. Water phase holdup values are complimentary to the values found for air phase holdup as expected. The experiments with glass beads of average diameter 117.6 μm are performed for the solids concentration of 104 kg/m^3 with results shown in Figure 17B. No foaming was visible in the column and the gas phase holdup increased with increasing air velocity for two- and three-phase systems. The effect on liquid holdup of solids is quite small.

A number of correlations have been proposed for the estimation of gas holdup in two-phase systems and most of these are summarized by Shah et al.[36] and Smith et al.[35] Some of the successful correlations for air-water system are due to Hughmark [12] Akita and Yoshida [13], Kumar et al. [14] Hills [15], Hikita et al.[16], Reilly et al.[17] and Smith et al. [18]. These are listed in Table 1 and computed values of average air holdup are compared with the experimental data in Figure 14. The nonmontonic variation of $\bar{\epsilon}_g$ with U found mostly for increasing U and sometimes with decreasing U, foam being present in both the cases, is qualitatively reproduced by the correlation of Kumar et al.[14] only. A detailed examination of the data belonging to individual runs revealed that the correlations of Hughmark [12] and Reilly et al.[17] are quite successful in reproducing the monotonic variation of $\bar{\epsilon}_g$ over the entire range of U values. Smith et al. [18] correlation obtained by modifying the Hughmark[12] correlation for three-phase systems leads to values which are similar to those obtained on the basis of Hughmark correlation as expected. Hills correlation[15] leads to somewhat higher values while those of Hikita et al.[16], and Akita and Yoshida [13] yield somewhat lower values than the experimental values.

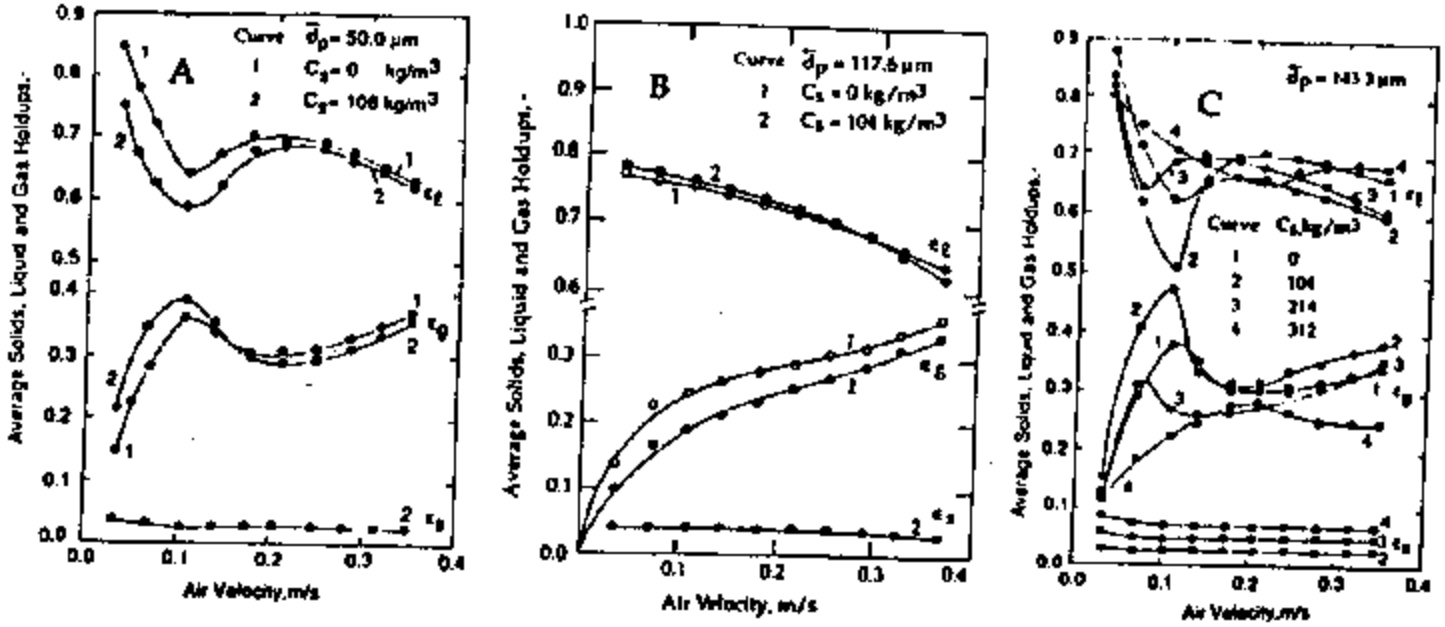

Fig. 17. Variation of average solids, liquid and gas holdup values as a function of decreasing superficial air velocity for different solids concentration (C_s) in the bubble column with a coaxial heat transfer probe at 294K for glass beads of three different average sizes (d_p).

The experimental data of air holdup with finite water flow velocities, $\bar{\epsilon}_g$ shown in Figure 15 are compared with the correlations of Hughmark[12] and Hills[15] as listed in Table 1. The qualitative variation of $\bar{\epsilon}_g$ with U for both the correlations is in general accord with the experimental findings. Both the correlations, however, overestimate the experimental data. The degree of disagreement does not seem to be dependent on the magnitude of V. Further, the predictions based on Hughmark[12] correlation are consistently in better agreement than those based on the correlation of Hills [15]

Thus based on our data for the air-water system for semi-batch and continuous modes of operation, it appears that the simple correlation of Hughmark [12] in the nonfoaming regime is most reliable for estimating the air holdup.

TABLE 1

Correlations of average air holdup for air-water system.

Investigator	Correlation*
Semi-batch operation	
Hughmark [12]	$\bar{\epsilon}_g = [2 + (0.35/U)]^{-1}$
Akita and Yoshida [13]	$\bar{\epsilon}_g/(1 - \bar{\epsilon}_g)^4 = 0.20\, Bo^{1/8}Ga^{1/12}Fr$
Kumar et al.[14]	$\bar{\epsilon}_g = 0.728U' - 0.485U'^2 + 0.0975U'^3$ where $U' = U[\rho_w^2/\{\sigma(\rho_w - \rho_a)g\}]^{1/4}$
Hills[15]	$\bar{\epsilon}_g = U\,[0.24 + 4.0\bar{\epsilon}_g^{1.72}]^{-1}$
Hikita et al. [16]	$\bar{\epsilon}_g = 0.672(U\rho_w/\sigma)^{0.578}(\mu_a^4 wg/\rho_w\sigma^3)^{0.131}(\rho_a/\rho_w)^{0.062}(\mu_a/\mu_w)^{0.107}$
Reilly et al[17]	$\bar{\epsilon}_g = 0.009 + 0.296U^{0.44}\rho_w^{-0.98}\sigma^{-0.16}\rho_a^{0.19}$
Smith et al [18]	$\bar{\epsilon}_g = [2.25 + (0.379/U)\mu_w^{0.016}]^{-1}$
Continuous operation	
Hughmark [12]	$U = \bar{\epsilon}_g[(U/\bar{\epsilon}'_g) - (V/1 - \bar{\epsilon}'_g)]$
Hills[15]	$(U/\bar{\epsilon}'_g) - (V/1 - \epsilon'_g) = 0.24 + 4.0\bar{\epsilon}'^{172}_g$

*All quantities are in SI unit system,

TABLE 2

Expressions for heat transfer coefficient in bubble columns.

Investigator	Expression*
Fair et al. 19	$h_w = 8850U^{0.22}$
Hikita et al. 26	$\frac{h_w}{\rho_w C_{pw} U}\left(\frac{C_{pw}\mu_w}{k_w}\right)^{2/3} = 411\left(\frac{U\mu_w}{\sigma}\right)^{-0.851}\left(\frac{\mu_w^4 g}{\rho_w \sigma^3}\right)^{0.308}$
Deckwer 21	$St = 0.1\,(ReFrPr^2)^{-0.25}$
Joshi et al. 22	A. Analogy with mechanically agitated contactors
	$\frac{h_w D_c}{k_w} = 0.48\left[\frac{D_c^{1.33} g^{0.33}\left(U - \bar{\epsilon}_g V_{b\infty}\right)^{1/3}\rho_w}{\mu_w}\right]^{0.66}\left(\frac{C_{pw}\mu_w}{k_w}\right)^{1/3}$
	B. Analogy with flow through pipes
	$\frac{h_w D_c}{k_w} = 0.087\left[\frac{D_c^{1.33} g^{1/3}\left(U - \bar{\epsilon}_g V_{b\infty}\right)^{1/3}\rho_w}{\mu_w}\right]^{0.8}\left(\frac{C_{pw}\mu_w}{k_w}\right)^{1/3}$
Zehner 23	$h_w = 0.18(1-\bar{\epsilon}_g)\,[k^2_w \rho^2_w C_{pw} V_c / f\mu_w]^{1/3}$
	where $f = d_b\,(\pi/6\bar{\epsilon}_g)^{1/3}$
	$V_c = \left[\frac{1}{2.5}\left(\frac{\rho_w - \rho_a}{\rho_w}\right) g D_c U\right]^{1/3}$
	and $\bar{\epsilon}_g = U/[0.25 \exp(5\bar{\epsilon}_g)]$
Present work	$\frac{h_w}{\rho_w C_{pw} U}\left(\frac{C_{pw}\mu_w}{k_w}\right)^{2/3} = 271\left(\frac{U\mu_w}{\sigma}\right)^{-0.851}\left(\frac{\mu_w g}{\rho_w \sigma^3}\right)^{0.308}$

*All quantities are in SI unit system.

HEAT TRANSFER DATA AND DISCUSSION

The heat transfer coefficient, h_w, between the heated section of area A of the probe at a temperature T_s and the surrounding air-water dispersion at temperature T_c is obtained from the relation

$$Q = h_w A(T_s - T_c). \qquad (6)$$

Here Q is the power fed to the electrical heater. h_w is measured here as a function of U and V, and further its dependence is investigated on Q and h. For the latter purpose, the heat transfer probe is located in three different regions viz., lower (h = 57.2 cm), middle (h = 87.5 cm) and upper (h = 118.1 cm), of the bubble column.

The heat transfer coefficient between the middle region of the probe and the air-water dispersion is measured as a function of U by Saxena et al, [4] and Saxena and Verma[10] Great care is exercised in establishing the values of T_s and T_c in eqn. (3). Seven thermocouples measure the temperature distribution on the probe surface and the standard deviation varies between 1.1 to 1.4. T_c is obtained by establishing the radial temperature profile and it is determined by a probe having six thermocouples located at 0, 2, 5, 10, 15 and 20 mm from its tip. These measurements reveal that temperature measured at 20 mm from the probe surface gives a good estimate of T_c. The standard deviation in the value of T_c varies between 0 and 0.5. A series of experiments is conducted to estimate the influence of thermal flux (Q/A) on h_w when all the other variables are held constant. The electrical power feed to the heater is varied between 0.456 and 0.943 kW when h_w varied by an average amount of 1.1 percent only. The corresponding column temperature is 312K, air velocity is 34.4 cm/s and mean h_w is 5.91 KW/m^2K. This observation is also in conformity with the earlier measurement of Saxena and Vadivel [3] with a tube bundle.

Measured values of h_w in the lower and upper region of the column are shown in Figure 18A and B as a function of time for several constant values of the air velocity. During the course of measurement, the column temperature increases with time and the increase is more for lower values of gas velocity. The approximate values of temperatures at different instants are indicated in the figure. At a constant column temperature, h_w assumes its steady state value within a few minutes, less than four minutes and more like two minutes. The rising h_w value with time, particularly evident at lower air velocities, is attributed to the rising temperature of the air-water dispersion in the column.

The steady-state h_w values as read from Figure 18 and the earlier values for the middle column region [4, 10] are plotted in Figure 19 as a

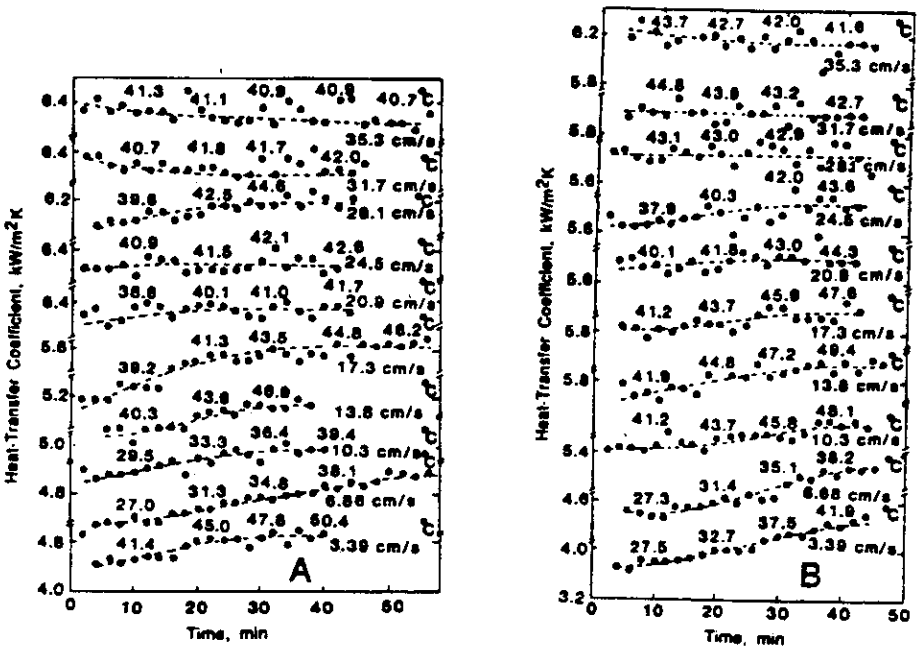

Fig. 18. Variation of the heat transfer coefficient with time at different air velocities. Heater is located at 57.2 cm (A, lower region) and 118.1 cm (B, upper region) above the distributor plate.

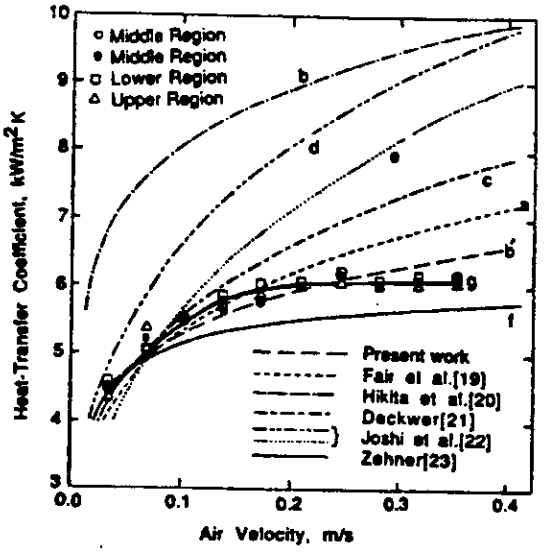

Fig. 19. Comparison of the experimental heat transfer coefficient for the air-water system with those predicted on the basis of different correlations and models as a function of air velocity at 315K.

function of U. The continuous thick line curve g represents the recommended h_w values. It is seen that the h_w values increase with the increase in U initially but then attain a constant value for air velocities greater than 25 cm/s. The scatter in the four sets of h_w values is generally less than ± 2 percent and therefore it is inferred that the variation of h_w along the column axis is negligibly small and can be neglected at least for operating conditions and system parameters of the present investigation.

A series of experiments is conducted to establish the influence of low water flow velocity on h_w. The measured h_w values as a function of time for V= 6.8 mm/s are shown in Figure 20A and V = 11.9 mm/s in Figure 20B. In both the cases, several values of U are arbitrarily chosen which maintain the air-water dispersion in an apparent state of churn-turbulent regime. Because not enough heat is removed from the system by the exiting gas, the column temperature exhibits a slow increase with time. The heat removed by circulating water is also small due to its low flow rate. In the figure several values of column temperature are shown for each U. In the light of our earlier comments, these h_w values are to be regarded as steady state values.

The h_w values as read from Figure 20A and 20B at 307 ± 1K are shown plotted in Figure 21. For V = 0, the measured h_w values are also shown. The influence of water flow velocity in the range of present measurements seem to be negligibly small as the scatter is always within the range of experimental uncertainty in h_w.

A detailed error analysis revealed that the maximum uncertainty in our h_w values is about 4.2 percent.

The present heat transfer coefficient measured values are compared with the correlations of Fair et al. [19] and Hikita et al. [20] and model predictions of Deckwer [21], Joshi et al. [22] and Zehner[23] in Figure 19. These expressions of h_w are listed in Table 2. A more extensive tabulation is given by Smith et al. [35] and Steff and Weinspach [24]. Fair et al.[19] correlation is simple and is developed on the basis of data for air-water system at 300 K in columns of diameter 45.67 cm and 106.7 cm fitted with air rings. h_w was measured for the column wall and the air-water dispersion in the former, and for a forty-two 3.8 cm diameter tube bundle for the latter. They, however, proposed the correlation based on their data for U values up to about 5 cm/s. The predicted values based on this correlation are shown in Figure 19 by curve a. It is seen that the calculated values are in reasonable agreement with the experimental values up to about 20 cm/s air velocity. As the air velocity is further increased the disagreement between the two sets of values increases and is about 13.5% at the highest air velocity of 35 cm/s.

Hikita et al.[20] correlation is developed on the basis of data (295 to 318K)for a wider range of air velocity values (5.3 to 34 cm/s) and several liquids having widely different values of viscosity and surface tension. Predictions based on this correlation (curve b) are consistently greater than our present h_w values, the disagreement increasing with gas velocity and is

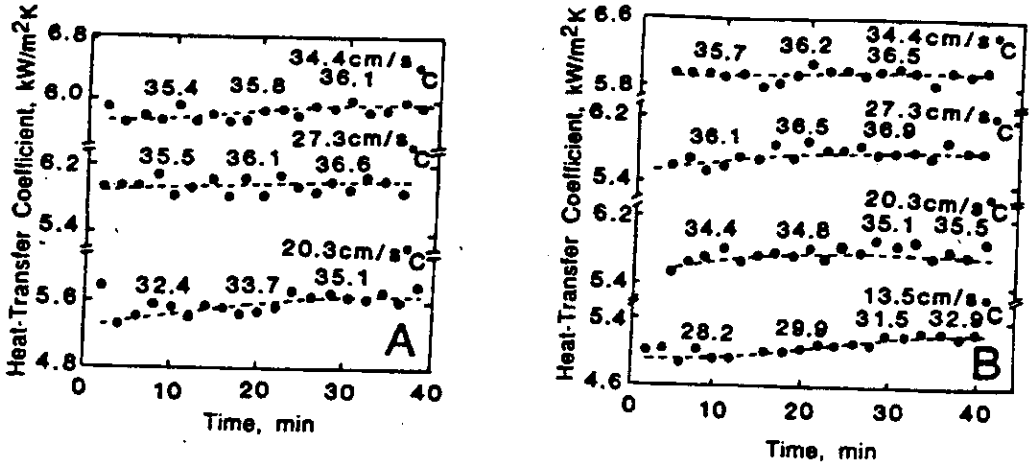

Fig. 20. Variation of the heat transfer coefficient with time at the water flow velocity of 6.8 mm/s (A), and 11.9 mm/s (B) for different air velocities.

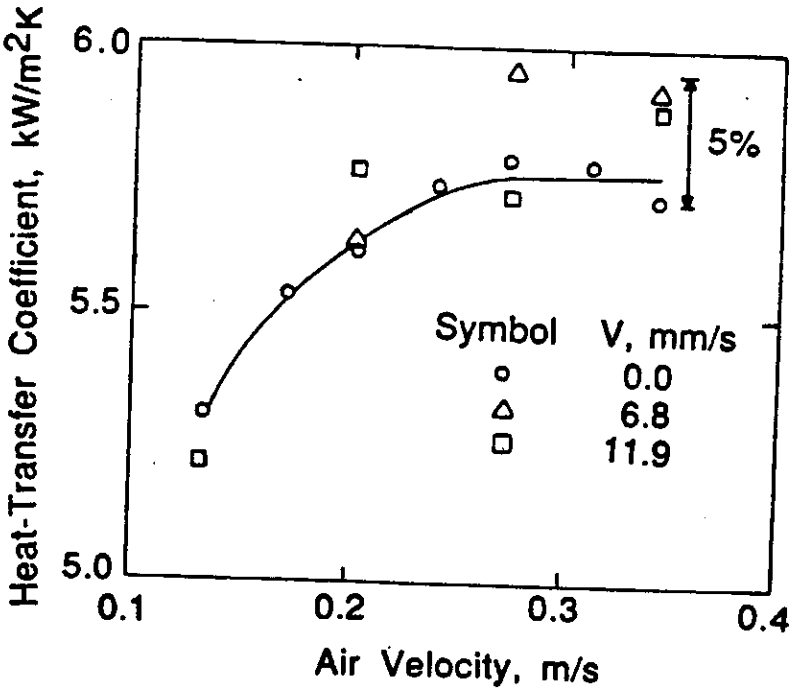

Fig. 21. Variation of the heat transfer coefficient at 307K with air velocity at different water flow velocities.

about 57% at the highest gas velocity. As a further check of the validity of this correlation we fitted our data and obtained the relation also listed in Table 2. Computed values of h_w based on this relation are also shown in Figure 19 by curve b. It should be noted that this relation, in general, does not have the ability to reproduce the qualitative trend of h_w to be constant at higher gas velocities.

Deckwer [21] examined a number of correlations which expressed Stantan number as a function of the product of Reynolds number, Froude number and (Prandtl number)^x, where x varied between 1.94 and 2.5. Further he considered following Kast [25] that the radial component of fluid velocity produced by the axial movement of bubble is an important parameter for heat transfer between the surface and the two-phase dispersion, and the Higbie[26] surface renewal model mimics the heat transfer process. The final form of his correlation in nondimensional form on the basis of experimental data is reproduced in Table 2. This relation is valid only up to about 10 cm/s of air velocity. Values based on this relation are displayed as curve c in Figure 19. The reproduction of experimental data is adequate up to U = 10 cm/s, and the computed values systematically diverge from the experimental values as the air velocity increases. The maximum disagreement is about 26% at the highest gas velocity. In view of the nature and magnitude of disagreement, it is inferred that the extrapolation of this correlation is not valid at air velocities greater than 10 cm/s. Joshi et al. [22] attributed this deficiency of the theory to the assumption that all the gas energy is dissipated in the liquid to create turbulence.

Joshi and Sharma[27] have argued that the input gas energy is dissipated and consumed in various ways and only less than 10% is used to create liquid motion in the bubbly flow regime. Based on a circulation cell model, they[27] have derived the following relation for the average liquid circulation velocity in a bubble column:

$$V_c = 1.31\left[gD_c\left(U - \bar{\epsilon}_g V_{b\infty}\right)\right]^{1/3} \qquad (7)$$

According to Joshi et al.[22] the enhancement of heat transfer from an immersed surface in a bubble column is due to the liquid circulation and they proposed two correlations which are reported in Table 2 based on analogies with mechanically agitated contactors and with flow through pipes. Predictions based on these two correlations are shown as curves d and e respectively in figure 19. In these computations $V_{b\infty}$ is taken as 0.23 m/s following Joshi and Sharma[28] which is based on Calderbank[29] work for bubbles of diameters in the range 6 to 7.2 mm and U in the range 5 to 30 cm/s. $\bar{\epsilon}_g$ is estimated from the relation developed by Mashelkar[30] for the air-water system. Both sets of computed values are systematically greater than the experimental values, the divergence is more pronounced for the

curve d (correlation A) than for the curve e (correlation B). At the highest gas velocity the differences in the calculated and experimental values are 47 and 30 percent for curves d and e respectively.

Zehner [23,31] has proposed a model based on the concept that a thermal boundary layer exists at the wall which is thinned at the places where bubbles are present. The length of the boundary layer is the same as the distance between successive bubbles, ℓ However, in the computation a constant value of 7mm is assumed. The heat transfer through this boundary layer is assumed to be the same as that over a flat heated plate. Zehner[23] proposed to use his correlation only up to about 10 cm/s and assumed h_w to be constant thereafter. Computed values based on this correlation are shown as curve f in Figure19. The increase in the computed h_w values for U greater than 10 cm/s is gradual but experimental data are underpredicted, the disagreement being 7.5% at the highest gas velocity.

The good agreement between our two earlier sets of h_w data [4,10] and the present data inspires confidence in the values and the trend indicated by curve g of Figure 19. On the other hand none of the available correlations and heat transfer models are capable of reproducing the experimental results. It is, therefore, interesting to compare the present experimental data with those available in the literature and the same is presented in Figure 23. Our data are displayed as curve a. The data of Kolbel et al.[32] at 313 K taken in columns of diameter 19.2 and 29.2 cm fitted with a porous plate distributor and a cylindrical heater of length 10 cm and diameter 3 cm are shown by curve b of Figure 22. In the overlapping air velocity range their data are in approximate agreement with the present results, the disagreement is about 10%. Kolbel et al [32] values are consistently smaller than our measured values. Fair et al.[19] data at 300 K referred to earlier is shown as curve c in Figure 22. One of their tubes in the bundle served as the heater. Their data at the highest gas velocity (5.0 cm/s) exhibit a scatter of about 7% and agrees with our data within about 5%. At lower gas velocities their data are significantly greater than those of Kolbel et al. [32] We think that the data of Kolbel et al. [32] are smaller than the actual values and probably it is due to the use of a relatively smaller heat transfer probe. The data of Burkel[33] referring to an immersed heater surface (dimensions not given), shown as curve d in Figure 22, are consistently smaller than the other measured values. The disagreement is about 22% with our values in the overlapping U range. Their value at the lowest air velocity is in agreement with that of Kolbel et al. [32] The reported data of Hart [34] at 344 K referring to the column wall of 9.9 cm diameter and equipped with a single nozzle (6.35 mm diameter) are shown as curve e in Figure 22. These data are consistently greater than all the other reported data sets.

Steff and Weinspach [24] employed a 19 cm diameter column with a

sintered plate distributor and measured h_w for the heated column walls at 313 K. Their data shown as curve f in Figure 22 are in good agreement with our values at higher velocities, the disagreement being always less than 5%. In the low velocity range, their data are greater than those of some other workers 32, 33, 35 and are smaller than those of Hart [34] and Hikita et al. [20] have measured h_w for column walls of diameters 10 and 19 cm equipped with single nozzle air spargers at 295-318 K. Their data shown as curve g in Figure 22 are systematically greater than all the other measured sets. Kast [25] has reported column wall (28.8 cm diameter) to air-water dispersion h_w values in the low velocity range. His values (curve h) are consistently greater than those of Kilbel et al [32] and are systematically smaller than those of Hart [34] and Steff and Weinspach.[24]

From the above discussion it is clear that large scatter exists in the h_w values for air velocities smaller than 2.0 cm/s. In the velocity range 2.0 to 36 cm/s the situation is relatively better. The measured values of Burkel [33] and Hikita et al.[20] are consistently and appreciably smaller and greater than the most probable values respectively. The present values are regarded in substantial agreement with the three remaining data sets [19,24,32]. However, precise measurements are needed as also the data in the higher velocity range. Further, these three data sets [19,24,32] suggest that h_w as determined for reactor wall and for an immersed heater surface are in good agreement with each other. This suggests that the geometry of the heat transfer surface probably plays only an insignificant role in the heat transport process in the higher air velocity range for small diameter reactors.

From the above discussion it is also clear that h_w has a distinct unique dependence on U and it is not even qualitatively reproduced by the existing correlations and models. This deficiency is due to the lack of proper understanding of the heat transfer mechanism between an immersed surface and the two-phase (gas-liquid) dispersion. To understand it we have performed experiments in which the unsteady state heat transfer process is investigated for the air-water system. To accomplish this the data acquisition system was programmed to compute h_w from measured surface and dispersion temperatures and record the same as a function of time at the sampling rate of ten h_w values per minute. One such record is shown in Figure 23 for five different air velocities. As seen in this figure, the column temperature exhibits a steady slow temperature rise over a period of fifty minutes. The net change depends on the gas velocity and the initial column

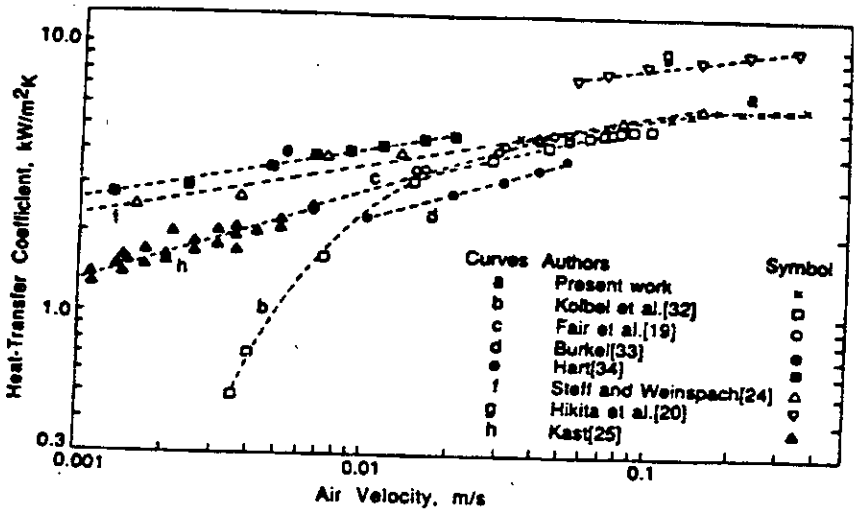

Fig. 22. Comparison of the present experimental heat transfer coefficient values for air-water system with those of the other workers as a function of air velocity.

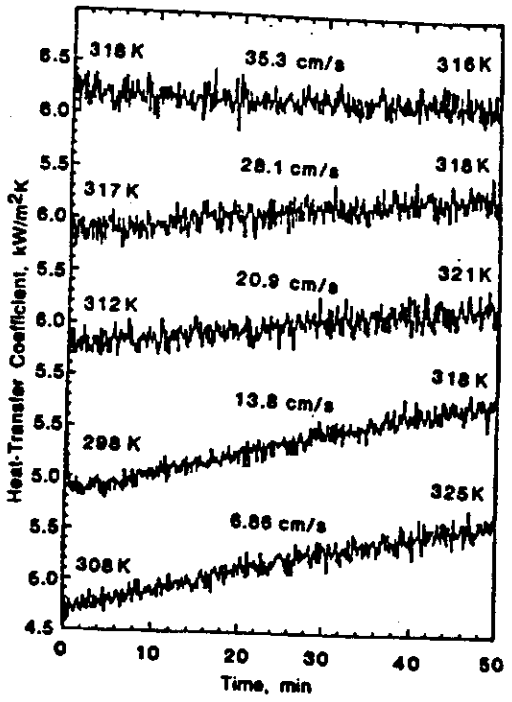

Fig. 23. Variation of heat transfer coefficient with time (and temperature) at various air velocities.

temperature relative to gas and ambient temperatures. It is important to note that the steady state is reached in about four minutes and thereafter any variation in h_w is to be attributed to the change in column temperature. It is also clear that h_w fluctuates continuously with time in a random fashion and the magnitude of maximum fluctuation seems to increase with increase in air velocity. The fluctuation which is 6.6% at 6.86 cm/s rises to 9.4% at 35.3 cm/s.

To gain more definitive understanding of the heat removal process it was considered desirable to record the local temperature of the heater surface as a function of time rather than the average as was done in Figure 23.
A pronounced variation of the local temperature with time and its periodicity will suggest the nature of phases in contact with the heater surface and their duration of stay and rate of replenishment i.e., their residence time and frequency. In Figure 24 are reported the records of local temperature of the heater surface as a function of time over a period of 10 s at the sampling rate of twenty readings per second. The experimental records correspond to different air velocities when a constant power is fed to the heater. Also shown in this figure (curve a) is the variation of local temperature when the heater surface is at the column temperature and the air is bubbled through the water column. The temperature variations of curves (b, c, and d) are to be evaluated in the background of variations implicit in curve a. It is clear that the local surface temperature does not exhibit wide fluctuations suggesting thereby that the nature of the phase in contact with it does not significantly change. From the curves c and d which correspond to the churn turbulent flow regime, it appears that there are two periodic patterns of temperature fluctuations. One having a time period of about 3 to 4 s and another of relatively smaller time period of about 0.6 to 1 s. The former corresponds to the periodic visit of dispersion elements at the probe surface element. These elements are of varying physical dimensions and that will explain the variation in the periodic time of this macroscopic activity. These dispersion elements have structures being constituted of a liquid element with several air bubble in it of varying sizes. This is responsible for the temperature fluctuations of smaller time period during the visit of a dispersion element at a particular probe site. The variations in the time period of this microscopic activity are to be attributed to the different mix of the pure phases (air bubble and water) in the dispersion element.

In the bubbly flow regime (curve b) the pattern of temperature fluctuation is different. The macroscopic activity mentioned above for churn turbulent flow is absent here and instead air bubbles and water elements periodically visit the heat transfer surface element. The time period of this activity will heavily depend upon the bubbling characteristics of the column

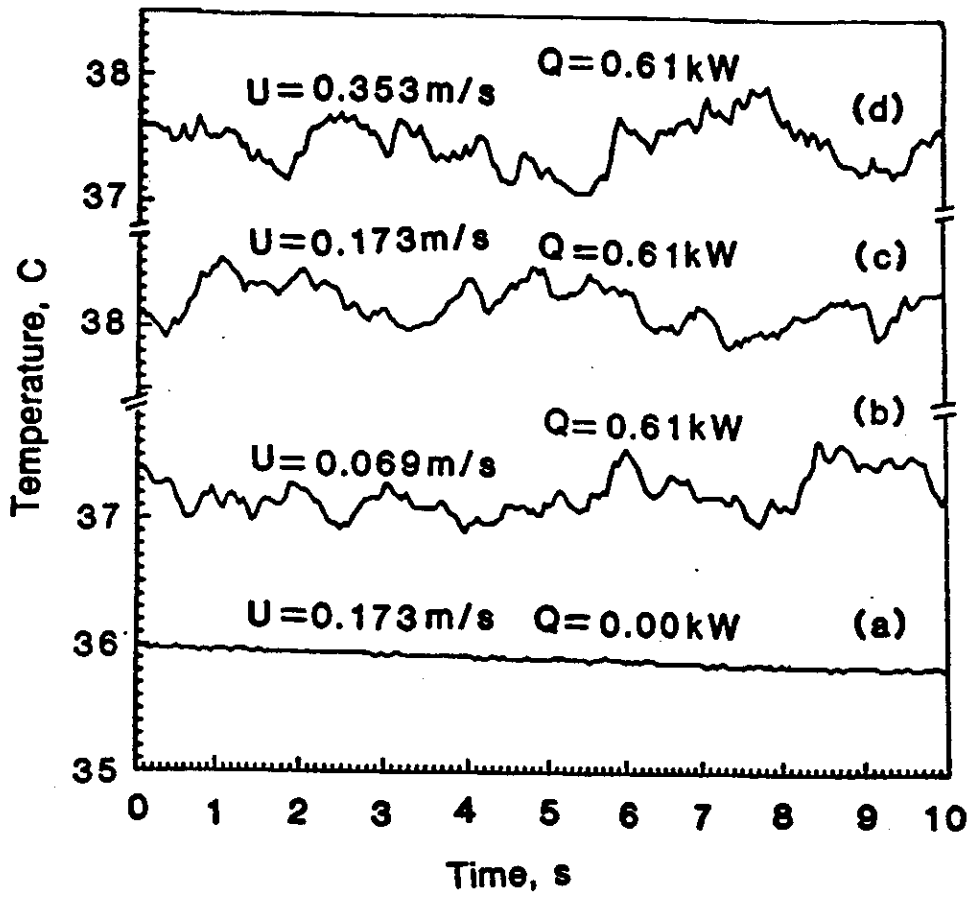

Fig. 24. Variation of local heater surface temperature with time at various air velocities (U).

and the bubble size distribution.

The above physical picture of heat transfer process is consistent with the qualitative features of h_w observed in the present investigations. The air holdup increases with increase in air velocity while h_w attains a constant value at higher air velocities. At low gas velocities, the liquid agitation increases with increase in gas velocity and hence h_w increases with increase in gas velocity. As the gas velocity is increased, the heat transfer rate becomes constant because any increase in the frequency of gas-liquid dispersion visit at the heat transfer survace does not significantly influence the heat removal rate in this gas velocity range. Any minor change in the heat transfer rate in this gas velocity range can also be balanced by the change in thermal properties of the dispersion element due to changes in its composition as the gas velocity is increased.

The above mentioned dependence of h_w on U is not consistent with the one likely mechanism of heat transfer in which the liquid and gas phases directly remove the heat from the immersed surface. For such a mechanism the heat transfer rate will increase with initial increase in gas velocity but must decrease at higher gas velocities due to increased population of gas bubbles at the probe surface.

Measured values of h_w for the air-water - glass beads systems of mean particle diameter as 50, 117.6 and 143.3 at various values of C_s as a function of air velocity is sketched in Figure 25. The data are also displayed in Figure 26 for all the three particles as a function of air velocity at a constant value of 104 kg/m^3 for C_s. From this study, the following conclusions may be drawn.

I. The heat transfer coefficient increases with increase in air velocity, the increase is rapid in the beginning but slows down as the air velocity is increased and approaches asymptotically to a constant value at higher air velocities.

II. The heat transfer coefficient values for the three-phase (air-water-glass beads) system are greater than for the corresponding two-phase (air-water) system under otherwise identical conditions. This difference increases with increase in solids concentration.

III. The effect of particle diameter on heat transfer coefficient appears to be negligibly small for the air-water-glass beads system and for glass particles in the range 50.0 to 143.3 μm.

With a view to understand the mechanism of heat transfer, the local temperature of the probe surface element is monitored over a time period at various air velocities. Such temperature history plots are dispayed in Figure 27. A slight upward drift of these plots with time is attributed to the increase in the probe surface temperature due to continuous accumulation of thermal

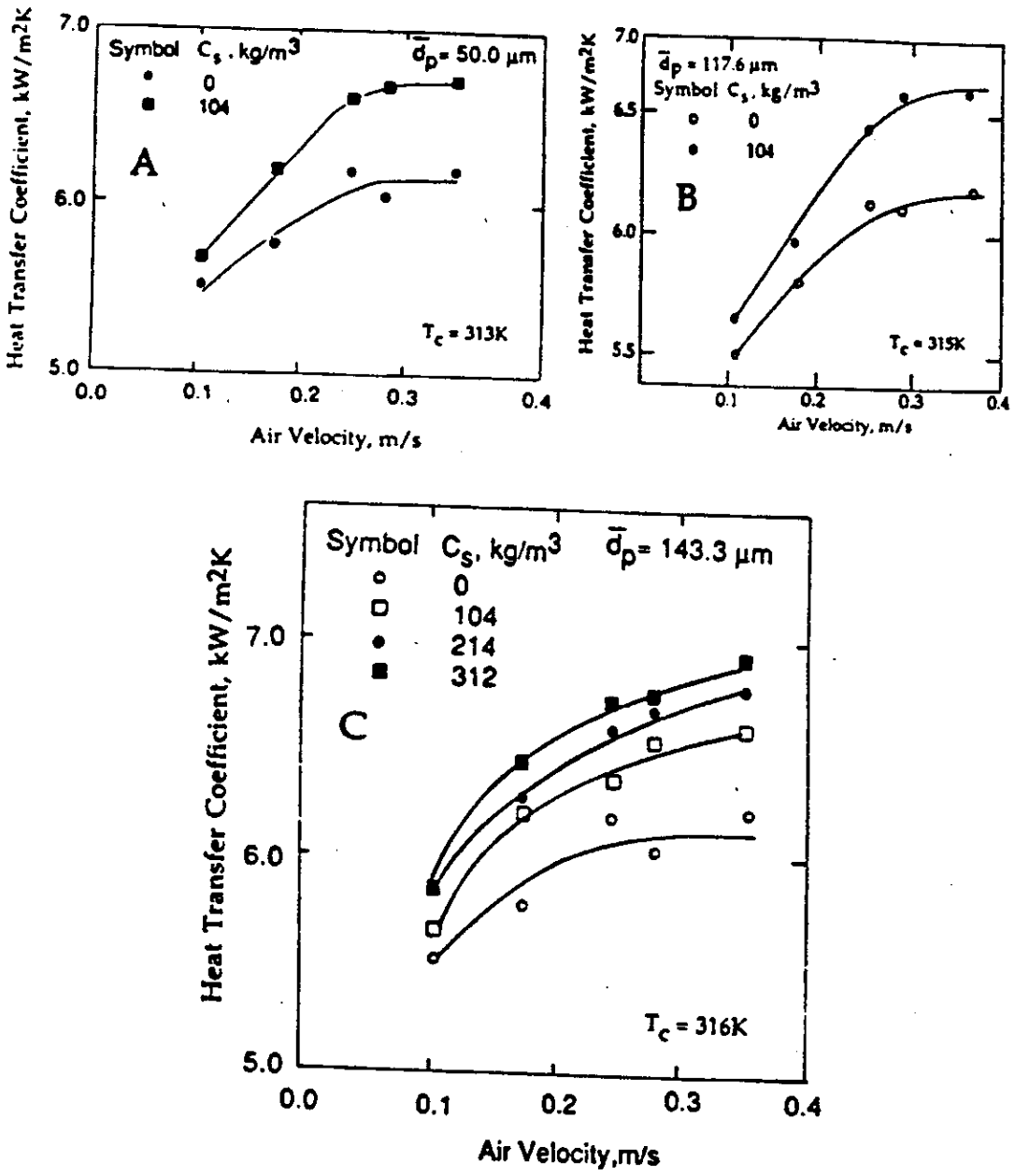

Fig. 25. Variation of heat transfer coefficient with superficial air velocity for slurries of different solids concentrations and particle sizes.

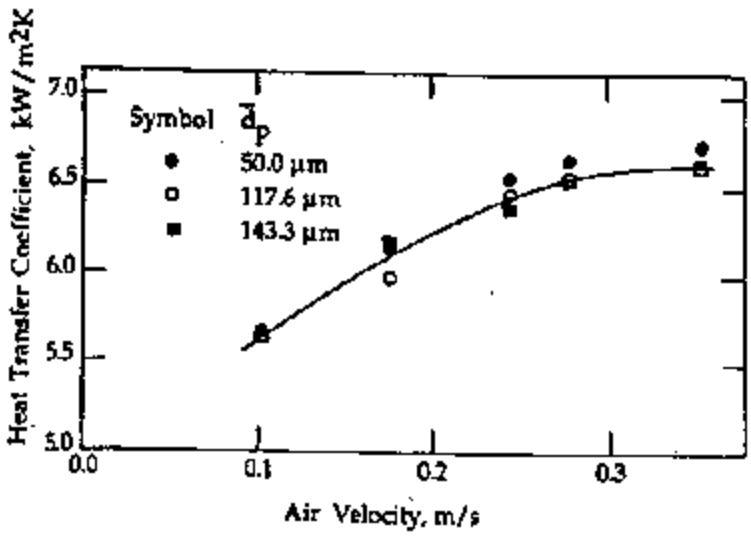

Fig. 26. Variation of heat transfer coefficient with superficial air velocity for slurries of different particle sizes at the solid concentration of 104 kg/m^3.

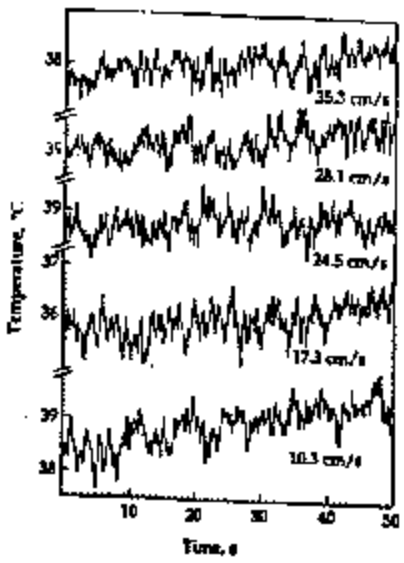

Fig. 27. Variation of the local temperature of the probe surface with time at various air velocities for glass beads of d_p = 117.6µmand C_s = 104 kg/m^3, are in mm.

energy in the system. The heat loss from the column wall and that by the air is less than the heat supplied to the probe heater. An approximate calculation shows the air residence time in the column to be about one second at the highest air velocity. The temperature history in Figure 27 is recorded at the rate of twenty readings per second. A visual exmination suggests that the temperature fluctuations are random and no systematic periodic change of temperature is evident. More detailed examination is being planned but based on the above discussion it would appear that the heat transfer surface is not visited by individual phases in a periodic fashion but instead probably dispersion elements contact the heater surface and remove the thermal energy.

ACKNOWLEDGEMENT

A number of researchers have contributed to the work included in this article. These are Mr. S. Shrivastava, Dr. R. Vadivel, Dr. A. K. Verma and Mr. A. C. Saxena. The able and devoted workmanship of Mr. W. Schindler, Mr. A. Sawczuk and Mr. J. Sitasz only enabled the design and fabrication of the experimental facilities. Lastly, thanks are due to Carolyne Schindler and Ferris Williams for typing this manuscript.

REFERENCES

1. S. C. Saxena amd S. Shrivastava, Heat Transfer Investigations in a Slurry Bubble Column, Indirect Liquefaction Contractor' Review Meeting, U. S. Department of Energy, Pittsburgh Energy Technology Center, pp. 177-187, 1986.
2. S. C. Saxena and R. Vadivel, Heat Transfer Investigations in a Slurry Bubble Column, Indirect Liquefaction Contractors' Review Meeting, U. S. Department of Energy, Pittsburgh Energy Techonology Center, pp. 365-391, 1987.
3. S.C. Saxena and R. Vadivel, Heat Transfer from a Tube Bundle in a Bubble Column, Int. Commun. Heat Mass Transfer, 15 (1988) 657.

4. S. C. Saxena, R. Vadivel and A. K. Verma Heat Transfer and Hydrodynamics of Bubble Columns with Internals, Proc. Third Latin American Congress on Heat and Mass Transfer, (Mexico), to be published.
5. S. C. Saxena, Heat Transfer from a Cylindrical Probe Immersed in a Bubble Column, under review for publication.
6. J. Zahradnik and F. Kastanek, Chem. Eng. Commun. 3 (1979) 413.
7. T. Maruyama, S. Yoshida and T. Mizushina, J. Chem. Eng. Japan, 14 (1981) 352..
8. D. B. Bukur and J. G. Daly, Chem. Eng. Sci., 42 (1987) 2967.
9. D. B. Bukur, D. Petrovic and J. G. Daly, Ind. Eng. Chem. Res., 26 (1987) 1087.
10. S. C. Saxena and A. K. Verma, Transport Phenomena in Multiphase Reactors, Proc. Int. Conf. on Advances in Chem. Eng., 1989, to be published.
11. S. C. Saxena. A. K. Verma, R. Vadivel and A. C. Saxena, Heat Transfer from a Cylindrical Probe in a Slurry Bubble Column, under review for publication.
12. G. A. Hughmark, Ind. Eng. Chem. Process Des. Dev., 6(1967) 218.
13. K. Akita and F. Yoshida, Ind. Eng. Chem. Process Des. Dev., 12(1973) 76.
14. A. Kumar, T. T. Dagaleesan, G. S. Laddha and H. E. Hoelscher, J. Chem. Eng., 54(1976) 503
15. J. H. Hills, Chem. Eng. J., 12(1976) 89.
16. H. Hikita, S. Asai, K. Tanigawa, K. Segawa and M. Kitao, Chem. Eng. J., 20 (1980)59.
17. I. G. Reilly, D. S. Scott, T. De Bruijn, A. Jain and J. Piskorz, Canadian J. Chem. Eng. 64(1986) 705.
18. D. N. Smith, W. Fuchs, R. J. Lynn and D. H. Smith, ACS Symp. Series No. 237, M. P. Dudokovic and P. L. Mills (Eds.), p. 125, 1984.
19. J. R. Fair, A. J. Lambright and J. W. Anderson, Ind. Eng. Chem. Process Des. Dev., 1(1962) 33.
20. H. Hikita, S. Asai, H. Kikukawa, T. Zaike and M. Ohue, Ind. Eng. Chem. Process Des. Dev.,20(1981) 540.
21. W. D. Deckwer, Chem. Eng. Sci., 35(1980)1 341.

22. J. B. Joshi, M.M. Sharma, , Y. T. Shah, C.P.P. Singh, M. Ally and G. E. Klinzing, Chem. Eng. Commun.,6(1980) 257.
23. P. Zehner, Int. Chem. Engng. 26(1986) 29.
24. A. Steff and P. M. Weinspach, Ger. Chem. Eng., 1(1979) 150.
25. W. Kast, Int. J. Heat Mass Transfer, 5(1962) 329.
26. R. Higbie, Trans. Am. Instn. Chem. Engrs., 35(1935) 365.
27. J. B. Joshi and M. M.. Sharma, Canadian J. Chem. Eng., 56(1978) 116.
28. J. B. Joshi and M. M. Sharma, Trans. Instn. Chem. Engrs., 57(1979) 244.
29. P. H. Calderbank, The Chem. Engr., No. 212 (1967) CE 209.
30. R. A. Mashelkar, Br. Chem. Eng., 15(1976) 1297.
31. P. Zehner, Int. Chem. Engng.,26(1986) 22.
32. H. Kolbel, W. Sienes, R. Maas and K. Muller, Chemie. Ing. Techn. 30(1958) 400.
33. W. Burkel, Chemie. Ing. Techn. 44(1972) 265.
34. W. F. Hart, Ind. Eng. Chem. Process Des. Dev., 15 (1976) 169.
35. D. N. Smith, G. J. Stiegel and J. A. Ruether, Chapter 15, in Encyclopedia of Fluid Mechanics, Volume 6, Gulf Publishing Co., Houston, 1986.
36. Y. T. Shah, B. G. Kelkar, S. P. Godbole and W. D. Deckwer, AIChEJ, 28 (1982) 353.